The Role of Imaging in the Detection and Management of COVID-19: A Review

Di Dong, Zhenchao Tang, Shuo Wang, Hui Hui, Lixin Gong, Yao Lu, Zhong Xue, Hongen Liao, Fang Chen, Fan Yang, Ronghua Jin, Kun Wang, Zhenyu Liu, Jingwei Wei, Wei Mu, Hui Zhang, Jingying Jiang, Jie Tian, *Fellow, IEEE*, and Hongjun Li

(Clinical Application Review)

Manuscript received April 12, 2020; revised April 20, 2020; accepted April 22, 2020. Date of publication April 27, 2020; date of current version January 22, 2021. This work was supported in part by the National Natural Science Foundation of China under Grants 81930053, 91959130, 81971776, 81771924, 81227901, 81671851, 81827808, 81527805, and 81971691, in part by the National Key R&D Program of China under Grants 2017YFA0205200, 2017YFC1308700, 2017YFC1309100, 2017YFA0700401, and 2016YFC0103803, in part by the Beijing Natural Science Foundation (L182061), and the Youth Innovation Promotion Association CAS (2017175), in part by the Hubei COVID-19 Emergency Grant (Z. Xue), in part by the Strategic Priority Research Program under Grant XDB32030200, and in part by the Scientific Instrument R&D Program under Grant YJKYYQ20170075 of the Chinese Academy of Sciences. *(Di Dong, Zhenchao Tang, Shuo Wang, Hui Hui, Lixin Gong, and Yao Lu contributed equally to this work.) (Corresponding authors: Jie Tian; Hongjun Li).*

Di Dong, Hui Hui, Kun Wang, Zhenyu Liu, and Jingwei Wei are with the School of Artificial Intelligence, University of Chinese Academy of Sciences, and also with the CAS Key Laboratory of Molecular Imaging, Institute of Automation, Chinese Academy of Sciences, Beijing, 100190, China.

Zhenchao Tang, Shuo Wang, Wei Mu, Hui Zhang, and Jingying Jiang are with the Beijing Advanced Innovation Center for Big Data-Based Precision Medicine School of Medicine and Engineering, Beihang University, and also with the Key Laboratory of Big Data-Based Precision Medicine (Beihang University)Ministry of Industry and Information Technology, Beijing, 100191, China.

Lixin Gong is with the College of Medicine and Biological Information Engineering School, Northeastern University, Shenyang, 110819, China (e-mail: gonglxhathaway@gmail.com).

Yao Lu is with the School of Data and Computer Science, Sun Yat-sen University, Guangzhou, 510275, China (e-mail: luyao23@mail.sysu.edu.cn).

Zhong Xue is with the Shanghai United Imaging Intelligence Co Ltd, Shanghai, 201210, China (e-mail: zhong.xue@united-imaging.com).

Hongen Liao is with the Department of Biomedical Engineering, School of Medicine, Tsinghua University, Beijing, 100084, China (e-mail: liao@tsinghua.edu.cn).

Fang Chen is with the Department of Computer Science and Engineering, Nanjing University of Aeronautics and Astronautics, Nanjing, 210016, China. (e-mail: chenfang@nuaa.edu.cn).

Fan Yang is with the Department of Radiology, Union Hospital, Tongji Medical College, Huazhong University of Science and Technology, Wuhan, 430022, China (e-mail: fyang@hust.edu.cn).

Ronghua Jin is with the Beijing Youan Hospital, Capital Medical University, Beijing, 100069, China (e-mail: 93353503@qq.com).

Jie Tian is with the CAS Key Laboratory of Molecular Imaging, Institute of Automation, Chinese Academy of Sciences, Beijing, 100190, China, and also with the Beijing Advanced Innovation Center for Big Data-Based Precision Medicine, School of Medicine and Engineering, Beihang University, Beijing, 100191, China (e-mail: tian@ieee.org).

Hongjun Li is with the Department of Radiology, Beijing Youan Hospital, Capital Medical University, Beijing, 100069, China (e-mail: lihongjun00113@126.com).

Digital Object Identifier 10.1109/RBME.2020.2990959

***Abstract*—Coronavirus disease 2019 (COVID-19) caused by the severe acute respiratory syndrome coronavirus 2 (SARS-CoV-2) is spreading rapidly around the world, resulting in a massive death toll. Lung infection or pneumonia is the common complication of COVID-19, and imaging techniques, especially computed tomography (CT), have played an important role in diagnosis and treatment assessment of the disease. Herein, we review the imaging characteristics and computing models that have been applied for the management of COVID-19. CT, positron emission tomography - CT (PET/CT), lung ultrasound, and magnetic resonance imaging (MRI) have been used for detection, treatment, and follow-up. The quantitative analysis of imaging data using artificial intelligence (AI) is also explored. Our findings indicate that typical imaging characteristics and their changes can play crucial roles in the detection and management of COVID-19. In addition, AI or other quantitative image analysis methods are urgently needed to maximize the value of imaging in the management of COVID-19.**

***Index Terms*—COVID-19, imaging, chest CT, artificial intelligence.**

I. Introduction

CORONAVIRUS disease 2019 (COVID-19), which is caused by the severe acute respiratory syndrome coronavirus 2 (SARS-CoV-2), emerged in December 2019 and rapidly developed into a global outbreak [1], [2]. COVID-19 presents as an acute respiratory tract infection syndrome and is highly infectious [3]. Critically ill patients with COVID-19 have a high mortality rate [4]. By April 20, 2020, more than 84,000 COVID-19 cases have been confirmed in China, and more than 2.30 million cases contracted the disease globally.

The typical clinical characteristics of COVID-19 cases include fever, respiratory symptoms, pneumonia, decreased white blood cell (WBC) count, and decreased lymphocyte count [5]–[7]. The reverse-transcription polymerase chain reaction (RT-PCR) testing is considered as the standard method for screening suspected cases [8], [9]. However, the sensitivity of RT-PCR screening is relatively poor in some situations. Thus, SARS-CoV-2 infection cannot be entirely excluded, even if RT-PCR results from a suspected patient are negative [10]–[12]. Therefore, medical imaging, in particular, chest computed tomography (CT), is often used as a complementary examination in the diagnosis and management of COVID-19. Typical imaging characteristics of lung in COVID-19 include lesions with ground-glass

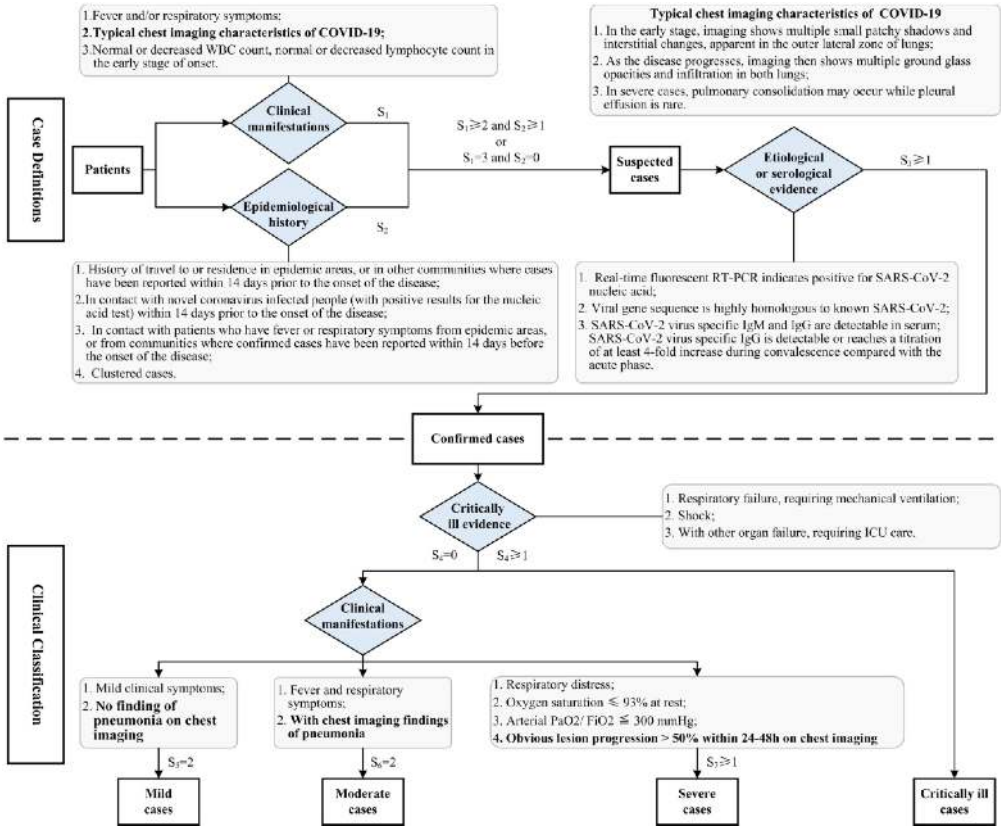

Fig. 1. The flowchart of case definitions and clinical classification of adult COVID-19 patients in China [9]. S_1-S_7: the number of entries that meet the conditions.

opacities (GGO), consolidation, bilateral patchy shadowing, pulmonary fibrosis, multiple lesions and crazy-paving pattern, and so on [13], [14]. These imaging interpretations played a key role not only in the diagnosis of COVID-19 but also in the monitoring of disease progression and the evaluation of therapeutic efficacy [15], [16].

The latest Chinese diagnosis and treatment protocol for COVID-19 (trial version 7) also highlights the value of imaging for detecting COVID-19 [9]. As shown in the flowchart of COVID-19 detection and staging of adult patients in China (Fig. 1), chest imaging has played an important role in both the case definitions and clinical classification.

Case definitions: For screening of the suspected cases, the epidemiological history and clinical manifestations of a patient are comprehensively analyzed, in which the chest imaging characteristics is adopted as one of the clinical manifestations [9]. Abnormal chest imaging characteristics of COVID-19 include multiple small patchy shadows and interstitial changes, more apparent in the peripheral zone of lungs (early stage), multiple GGO and infiltration in both lungs (progression stage), and pulmonary consolidation (severe stage). A suspected case with any positive etiological or serological results is confirmed as COVID-19.

Clinical classification: Confirmed COVID-19 cases are classified as mild, moderate, severe, or critically ill cases. The classifications of the first three types all involve the chest imaging. COVID-19 patients with mild clinical symptoms and with no sign of pneumonia on chest imaging are confirmed as mild cases, while patients with fever, respiratory symptoms, and chest imaging findings of pneumonia are categorized as moderate cases. Besides the respiratory distress, oxygen saturation, and arterial partial pressure of oxygen (PaO2)/fraction of inspired oxygen (FiO2), an adult patient with chest imaging showing obvious lesion progression >50% within 24–48 hours is managed as a severe case.

There are lots of studies investigating the imaging characteristics during the diagnosis, follow-up, and treatment of COVID-19 [5], [13], [17]. A comprehensive review of the role of imaging in the detection and management of COVID-19 is urgently needed. In this review, we searched Google Scholar, PubMed, and Web of Science using the keywords "coronavirus, or COVID-19, or 2019-nCoV, or pandemic" and "imaging" for alternative literature published before April 20, 2020. The search resulted in more than 1,000 publications. We then carefully selected the most appropriate articles about the imaging of COVID-19.

In Section II, we will first introduce the imaging characteristics used for the detection of COVID-19. Then, the change of imaging characteristics during the follow-up and the treatment of COVID-19 patients is described in Section III. The quantitative analysis could maximize the effectiveness of imaging, and the AI-based image analysis is conducted in Section IV. Finally, we provide a thorough discussion of key findings in Section V with a conclusion in Section VI.

II. Imaging Modalities in Diagnosis Of COVID-19

Medical imaging is a useful supplement to RT-PCR testing for the diagnosis of COVID-19. Typical imaging characteristics, especially the CT characteristics, are found in COVID-19 patients. In the following subsections, we will introduce CT and other imaging modalities in diagnosis of COVID-19.

A. The CT Characteristics in Diagnosis of COVID-19

1) CT Characteristics of Typical COVID-19: Chest CT scan of COVID-19 patients could be evaluated for the following characteristics [5], [13], [17]–[20]: (1) presence of GGO; (2) presence of consolidation, (3) laterality of GGO and consolidation; (4) number of lobes affected by GGO or consolidative opacities; (5) degree of each lung lobe involvement in addition to the overall extent of lung involvement; (6) presence of nodules; (7) presence of pleural changes such as pleural effusion or pleural thickening; (8) presence of thoracic lymphadenopathy; (9) airway abnormalities; (10) axial distribution of disease; (11) presence of underlying lung disease such as emphysema or fibrosis; and other abnormalities including linear opacities and opacities with a crazy-paving pattern.

The above mentioned CT characteristics have got extensive attention from the clinicians [21]. The typical CT characteristics for four COVID-19 cases are shown in Fig. 2. Table I shows several studies about the CT characteristics in COVID-19.

GGO, defined as hazy increased lung attenuation with preservation of bronchial and vascular margins [22], [23], is the most common early finding of COVID-19 on chest CT. Guan *et al.* [5] found that 56.4% COVID-19 patients had GGO in chest CT imaging. Ai *et al.* [10] also reported that GGO was one of the main CT signs of COVID-19 patients, even in suspected cases with initial negative RT-PCR testing. Han *et al.* [24] pointed out that early CT findings are multiple patchy pure GGO with or without consolidation involving multiple lobes, mainly in the peripheral zone, accompanied by a halo sign, vascular thickening, or air bronchogram signs. Salehi *et al.* [25] performed a systematic review of imaging findings of COVID-19 and found that GGOs are prone to increase in number and size, and often progressively transform into multifocal consolidative opacities and septal thickening in the intermediate stage of the disease. Xu *et al.* [26] found that the density of lung lesion in COVID-19 was mostly uneven with GGO as the primary presentation accompanied by partial consolidation and fibrosis. Wu *et al.* [27] investigated 80 patients diagnosed with COVID-19 and found that 73% of the patients with clinical manifestations (e.g., cough and fever) demonstrated multiple typical imaging features like GGO, interlobular septal thickening, and consolidation. Similar features and enlargement of vascular were also reported in Zhao et al's study [28].

Besides GGO, bilateral patchy shadowing is one of the most common radiologic findings on chest CT [5], [16], [25]. Two studies have investigated the percentage of bilateral involvement in patients with COVID-19 [3], [17]. They studied the degree of involvement in disease classification of the five lung lobes and found up to almost 100% bilateral involvement of them for patients with COVID-19. In a study of 41 patients in Wuhan,

TABLE I
Several Studies of CT Characteristics in COVID-19

Ref	Data Source	Number of patients	CT characteristics
Guan et al. [5]	552 hospitals in China	1099 COVID-19 patients, 975 of them had CT	**CT signs of COVID-19:** GGO (550/975, 56.4%) ; Local patchy shadowing (409/975, 41.9%); Bilateral patchy shadowing (505/975, 51.8); Interstitial abnormalities (143/975, 14.7%).
Ai et al. [10]	Tongji Hospital, Wuhan, China	1014 suspected patients, 601of them had positive RT-PCR testing	**CT signs of suspected COVID-19:** Positive chest CT signs (888/1014, 88%); GGO (409/888, 46%); Consolidations (447/888, 50%); Bilateral chest CT signs (801/888, 90%). **CT signs of 413 RT-PCR negative suspected COVID-19:** Positive chest CT signs (308/413, 75%); Bilateral lung lesions (256/308, 83%); GGO (126/308, 41%); Consolidations (172/308, 56%).
Zhao et al. [28]	Radiology Quality Control Center, Hunan, China	101 COVID-19 patients	**CT signs of COVID-19:** GGO (87/101, 86.1%); Mixed GGO and consolidation (65/101, 64.4%); Vascular enlargement in the lesion (71.3%); Traction bronchiectasis (53/101, 52.5%).
Bai et al. [29]	7 hospitals from Hunan Providence, China; and Rhode Island Hospital in Providence, RI, USA	219 COVID-19 patients and 205 patients with viral pneumonia	**CT signs COVID-19 *vs.* non-COVID-19:** Peripheral distribution (80% *vs.* 57%); GGO (91% *vs.* 68%); Fine reticular opacity (56% *vs.* 22%); Vascular thickening (58% *vs.* 22%); Reverse halo sign (11% *vs.*1%).
Zhu et al. [30]	First Affiliated Hospital of University of Science and Technology of China, Anhui, China	32 COVID-19 patients and 84 non-COVID-19 patients	**CT signs of COVID-19:** Pneumonia (30/32, 94%); Bilateral involvement (29/32, 91%); GGO (15/32, 47%); Spider web pattern (4/32, 13%).
Li et al. [31]	Second Affiliated Hospital of Chongqing Medical University, Chongqing, China	83 COVID-19 patients	**CT signs of COVID-19:** GGO (81/83, 97.6%); Linear opacities (54/83, 65.1%); Consolidation (53/83, 63.9%); Interlobular septal thickening (52/83, 62.7%); Crazy-paving pattern (30/83, 36.1%).

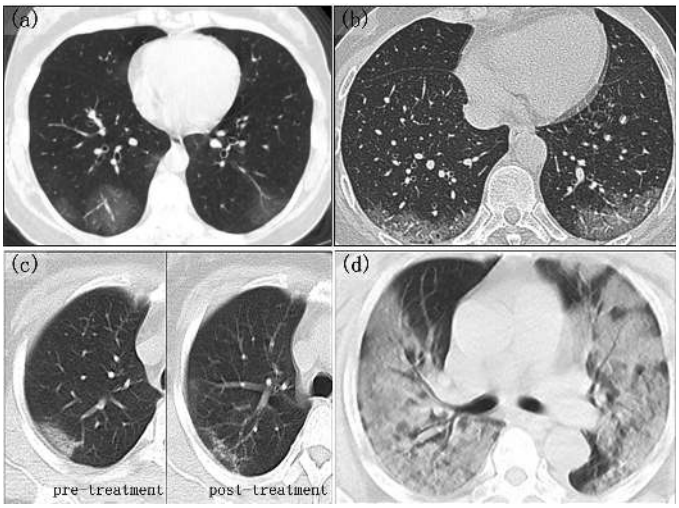

Fig. 2. Four examples of COVID-19 patients from Beijing Youan Hospital. (a) Early stage patient: Female, 44 years old, fever for 3 days, body temperature 38.3 °C, fatigue, cough. CT characteristics: Multiple pulmonary lobules involved, sub-pleural focal GGO accompanied by bronchial passage, thickened blood vessels, no mutual fusion or consolidation opacity. (b) Progression stage patient: Female, 56 years old, fever for 2 days, no cough, body temperature 37.3 °C. CT characteristics: Multiple pulmonary lobules or involvement of lung segments in the advanced stage, localized GGO accompanied by bronchi running under the pleura, thickened blood vessels, merged pulmonary lobule opacities, and local consolidation opacity. (c) Outcome stage patient: Female, 30 years old, fever and cough for 5 days. CT characteristics: Multiple focal high-density opacities in both lung fields on the 5th day of onset (pre-treatment); absorption improved on the 8th day of onset (post-treatment), showing streaky opacity only. (d) Severe (critically ill stage) patient: Male, 53 years old, fever for 3 days with a dry cough, body temperature up to 39 °C. CT characteristics: The consolidation of the two lungs is known as "white lung", high-density opacity occurs due to the alveoli being filled with a large number of phagocytes and neutrophil fragments, losing gas exchange capacity, and becoming consolidated.

China, Huang *et al.* [32] claimed that abnormalities in chest CT images were detected among all patients, and most patients had bilateral involvement. The typical CT findings of ICU patients were bilateral multiple lobular and subsegmental areas of consolidation.

Consolidation and pulmonary fibrosis are also typical CT signs in the late stage of COVID-19. In a study involving 51 COVID-19 patients, Song *et al.* [33] concluded that lesions with consolidation could serve as either a marker of disease progression or of more severe disease. Consolidation was found to be more common in pregnant women [22]. Sun *et al.* [34] found that COVID-19 infection could increase the risk of pulmonary fibrosis, and they suggested that pulmonary fibrosis could become a critical complication in patients with COVID-19. Thus, it is important for clinicians to be alert to the occurrence of pulmonary fibrosis in COVID-19 patients.

Multiple lesions and crazy-paving pattern are also common in COVID-19 patients. Zhou *et al.* [35] found that, even on the initial CT scan, COVID-19 is more likely to manifest as multiple lesions rather than a single lesion. Moreover, in the early stage of the disease, the virus is more likely to invade the branches of the right inferior lobar bronchus and cause infection. The lesions showed a predominantly peripheral distribution, with the middle and lower zones and the posterior area of both lungs were significantly more involved. Li *et al.* [31] showed that 36% patients, especially the severe patients, have crazy-paving patterns in chest CT images, which could be a sign of the poor condition.

2) CT Characteristics in Asymptomatic COVID-19: Screening of patients with an asymptomatic or atypical presentation is an important aspect of controlling the spread of COVID-19. As a diagnosis tool, CT is also useful to explore the imaging characteristics of asymptomatic and atypical patients. Hao *et al.* [36] found that, when the initial RT-PCR results of some patients were negative, chest CT showed typical radiographic findings, including GGO and/or mixed consolidation. Ai *et al.* [10] also reported the CT signs (bilateral lung lesions, GGO, and consolidations) of suspected COVID-19 patients with negative RT-PCR testing. Similarly, Fang *et al.* [37] reported that the CT signs of asymptomatic COVID-19 pneumonia included bifocal extra-zonal, bilateral and multifocal distribution.

However, not all asymptomatic patients have typical radiographic signs. Hu *et al.* [38] collected a total of 24 asymptomatic patients in China who were confirmed to be positive for COVID-19 by RT-PCR. Of these 24 patients, 12 patients showed typical chest CT images, which included GGO shadows; 5 patients had fever, cough, fatigue, and other symptoms during hospitalization, with chest CT images showing atypical radiographic signs (e.g., striped shadows in the lungs). The remaining 7 patients showed normal CT images in addition to having no clinical symptoms. In the statistical analysis of the patients' clinical characteristics, the authors found that 7 patients with normal CT findings and no symptoms were significantly younger than the other patients (median age: 14.0 years old, $P = 0.012$). That study also confirmed that asymptomatic patients were contagious as well. Ling *et al.* [39] drew the same conclusions regarding the chest CT scans of asymptomatic patients: the authors retrospectively collected the data of 295 patients and found initial negative CT images in 49 patients. Of these 49 patients, 15 became positive after 3-6 days. The CT images of the other 34 patients showed persistent negative (after 3–14 days), and it should be noted that 4 of them did not show any clinical symptoms or imaging abnormalities. Therefore, not all asymptomatic patients have typical CT signs. The combination of chest CT imaging, RT-PCR, and close follow-up should be used to detect these asymptomatic COVID-19 patients.

3) Use of CT Characteristics for Discriminating COVID-19 Pneumonia From Other Pneumonia: The use of CT findings for discriminating COVID-19 pneumonia from other pneumonia has attracted considerable attention. Upon reviewing coronavirus cases associated with severe acute respiratory syndrome (SARS) and the Middle East respiratory syndrome (MERS), GGO and/or lung consolidation were typically characterized on chest CT, which is different from the characteristics of other viruses [40]. Similarly, the typical radiological features of COVID-19, multiple lobular GGO and subsegmental areas of consolidation are met more often [41]. Beyond that, most patients with COVID-19 pneumonia show bilateral involvement and multiple mottling, whereas the typical features of

non-COVID-19 pneumonia are patchy shadows or density increasing shadows [41]. Compared to other pneumonia, patients with COVID-19 are more likely to exhibit CT abnormalities characterized by peripheral distribution, fine reticular opacity, vascular thickening, and reverse halo sign, but are less likely to have significant levels of central-peripheral distribution, pleural effusion, and lymphadenopathy [29]. As the disease progresses, there is rapid infiltration in lobes of COVID-19 patients as suggested by sequential CT scans [30]. A part of late infection stage COVID-19 patients also exhibits spider web and crazy-paving patterns [14], [41].

B. Other Imaging Techniques in COVID-19 Diagnosis

In addition to chest CT, other imaging modalities are also used as complementary of chest CT in the diagnosis of COVID-19, including positron emission tomography - CT (PET/CT), lung ultrasound, and magnetic resonance imaging (MRI). In the following sub-sections, a brief introduction of these imaging techniques is provided.

1) PET/CT: PET is a sensitive but invasive imaging method that plays an important role in evaluating inflammatory and infectious pulmonary diseases, monitoring disease progression and treatment effect, and improving patient management. Qin *et al.* [42] reported that lung lesions of patients with COVID-19 pneumonia were characterized by a high ^{18}F-FDG uptake, the lymph nodes were involved, and the disseminated disease was absent on ^{18}F-FDG PET/CT imaging. They suggest that ^{18}F-FDG PET/CT can play an auxiliary diagnostic role in COVID-19, especially in the early stage, when the differential diagnosis is difficult. In one case report, high uptake of ^{18}F-FDG was found in the lymph nodes and bone marrow by PET/CT evaluation [43]. Similarly, a high and significant ^{18}F-FDG uptake has been observed in patients with MERS-CoV infection [44]. In a letter to the editor, Deng *et al.* [45] suggested that FDG uptake may reflect non-specific inflammation or immune activation. Chu *et al.* [46] found that the SARS-CoV-2 infection caused inflammatory and significantly upregulated five inflammatory mediators. That may be why the COVID-19 patients had a high uptake of ^{18}F-FDG. Therefore, PET/CT can play an important role in identifying changes in uptake patterns and locations during viral exposure, and patients with higher FDG uptake in lesions may have a longer recovery period.

In contrast, another letter to the editor by Joob *et al.* [47], had a different view, stating that ^{18}F-FDG PET/CT is a more complex test than chest CT, and longer testing period for ^{18}F-FDG PET/CT examinations may increase risk of disease transmission. They conclude that further studies are needed to determine whether ^{18}F-FDG PET/CT is an appropriate testing modality for COVID-19.

2) Lung Ultrasound: As a non-invasive, radiation-free, and portable imaging method, lung ultrasound (LUS) allows for the initial bedside screening of low-risk patients, diagnosis of suspected cases in the emergency room setting, prognostic stratification, and monitoring of the changes in pneumonia [48]–[50]. Peng *et al.* [51] reported that lung ultrasonography could provide results comparable with chest CT for evaluation of COVID-19 pneumonia. For severe or critical patients, especially those admitted to the ICU and requiring ventilation, LUS is necessary for patient management and monitoring the effectiveness of treatments. More importantly, the use of LUS can reduce the exposure risk between infected patients and health care workers, and discriminate between low-risk and higher-risk cases. Bunosenso *et al.* [52] reported a confirmed case that LUS showed an irregular pleural line with small subpleural consolidations, areas of white lung and thick, confluent and irregular vertical artifacts (B-lines). For pregnant women with suspected COVID-19, chest CT examination should be avoided as much as possible due to the high radiation. As an alternative, Moro *et al.* [53] recommended that obstetricians and gynecologists could perform lung examination using LUS.

3) MRI: MRI is a powerful radiation-free imaging technique for visualizing soft tissues. However, it is not commonly applied to COVID-19 diagnosis due to a relatively long scanning time and high cost compared to CT and LUS. Nonetheless, the non-invasive MRI may help evaluate COVID-19 in children and pregnant women [54].

The infection of SARS-CoV-2 is mainly distributed in the lung, but three minimally invasive autopsies showed that the infection also involves in the damages of heart, vessels, liver, kidney, and other organs [55]. At the molecular level, Angiotensin-converting enzyme 2 (ACE2), the key host cellular receptor of SARS-CoV-2, has been identified in multiple organs. The study carried out by Chen *et al.* [56] confirmed that patients with basic heart failure disease showed increased ACE2 expression at both mRNA and protein levels and may have a higher risk of heart attack and critically ill condition. Similarly, cardiac MRI also showed cardiac involvements in patients with COVID-19, such as acute myopericarditis with systolic dysfunction [57]. At the RNA level, Zou *et al.* [58] identified other organs at risk like the esophagus, kidney, bladder, and ileum that are vulnerable to COVID-19 infection.

Due to excellent performance for visualizing structural and functional information of various soft organs, MRI could be used to study the vulnerability of different organs for a better understanding of the pathogenesis and mechanisms of COVID-19 infection. Meanwhile, similar to the studies of [59] and [60], where the ability of MRI, CT, X-Ray, and LUS for diagnosing pneumonia can be evaluated and compared, many researches can be done for COVID-19 patients to not only compare different modalities or their combinations but also systematically study the organ damages and mechanisms of the disease.

III. The CT Characteristics During the Follow-Up and Treatment of COVID-19

Follow-up CT scans are often performed for patients with COVID-19 to assess the progression or improvement during the disease course. Moreover, quantitative follow-up can also improve the recognition of imaging characteristics with radiologists and assisted them in making a quick and accurate diagnosis. In this section, we focus on the CT manifestations in different stages of COVID-19; the quantitative CT metric changes with

the advantage of COVID-19 progression are discussed; and the remission of lung lesions on CT images is depicted.

A. CT Manifestations in Different Stages of COVID-19

Follow-up CT checking images reveal temporal changes in imaging characteristics for COVID-19 [18], [22], [23], [32], [61]–[65]. By grouping COVID-19 patients based on disease courses, CT manifestations of lung lesions are analyzed based on different stages. Table II summarizes the related findings.

The disease stages are mostly divided according to the time after the onset of clinical symptoms. In [35], the disease was roughly divided as the early phase ($\leq$7 days) and advanced phase (8–14 days). In the early phase, the frequency of GGO with a reticular pattern, vacuolar sign, fibrotic streaks, a subpleural line, a subpleural transparent line, air bronchogram, bronchus distortion, and pleural effusion is very high. Bernheim *et al.* [18] divided the patients into early group (0-2 days), intermediate group (3-5 days), and late group (6-12 days). In the early group, no lung opacities or slight GGO were observed among the patients. GGO and consolidation were frequently observed in patients in the intermediate group. In the late group, in addition to GGO and consolidation, linear opacities and crazy-paving patterns were observed.

On the other hand, disease stages were divided into a more detailed description in the work of Pan [66] and Wang [67]. Pan *et al.* [66] divided patients into Stage-1 (0-4 days), Stage-2 (5-8 days), Stage-3 (9-13 days), and Stage-4 ($\geq$14 days). Patients in Stage-1 had GGO with partial crazy-paving pattern and consolidation. In Stage-2, the GGO extended to additional lobes, with increased crazy-paving pattern and consolidation. In Stage-3, consolidation became the main CT manifestation, and the GGO and crazy-paving patterns decreased. In Stage-4, the consolidation was partially absorbed without any crazy-paving pattern. Wang *et al.* [67] investigated temporal changes of chest CT characteristics, and divided the stages as $<$ 0 days, 0-5 days, 6-11 days, 12-17 days, 18-23 days and $\geq$ 24 days (Fig. 3). The lung lesions on CT images were predominantly manifested as GGO in most stages. In the earlier stages, each lung was divided into 3 zones: upper (above the carina), middle, and lower (below the inferior pulmonary vein) zones; each zone was evaluated for percentage of lung involvement on a scale of 0-4. They studied the median values of the total CT score and the number of zones involved as a function of time, and analyzed the temporal changes of the main CT patterns (GGO and consolidation). It can be drawn from previous studies that GGO was the main manifestation of COVID-19, especially in the early stages. With the progression of the disease, GGO gradually decreased, and consolidation became the increased pattern of lung lesions.

Many studies have reported an association between COVID-19 and the manifestation of clinical factors of RT-PCR results. Ai *et al.* [10] enrolled 1014 suspected COVID-19 patients and reported that there was a correlation between COVID-19 and imaging manifestation of clinical factors. In the initial group diagnosed as positive RT-PCR results, the authors reported that 60% of patients showed consistent CT features, including GGO, consolidation, reticulation/thickened interlobular septa, and nodules. Moreover, nearly all of the initial positive cases showed positive chest CT scans within a week. The findings revealed that chest CT detection is necessary to screen the suspected cases early. The authors also analyzed the CT images and serial RT-PCR assays, and found 60% to 93% of cases had the same manifestation of positive chest CT before the

TABLE II
SUMMARY OF THE CT MANIFESTATIONS OF COVID-19 IN DIFFERENT STAGES

Ref.	Stage	CT characteristics	Number of COVID-19 patients
Bernheim et al. [18]	Early group (0-2 days)	No lung opacities or GGO	36
	Intermediate group (3-5 days)	GGO and consolidation	33
	Late group (6-12 days)	GGO, consolidation, linear opacities and crazy-paving pattern	25
Zhou et al. [35]	Early phase ($\leq$7 days)	The frequency of GGO is significantly higher	40
	Advanced phase (8-14 days)	The frequency of GGO with a reticular pattern, vacuolar sign, fibrotic streaks, a subpleural line, a subpleural transparent line, air bronchogram, bronchus distortion, and pleural effusion is significantly higher	22
Pan et al. [66]	Stage-1 (0-4 days)	GGO with partial crazy-paving pattern and consolidation	24
	Stage-2 (5-8 days)	GGO extended to more lobes with more crazy-paving pattern and consolidation	17
	Stage-3 (9-13 days)	Consolidation as main manifestation with decreased GGO and crazy-paving pattern	21
	Stage-4 ($\geqslant$14 days)	Consolidation partially absorbed without any crazy-paving pattern	20
Wang et al. [67]	<0 days	Normal, or GGO and consolidation	10
	0-5 days	Predominant GGO with consolidation	79
	6-11 days	Predominant GGO with consolidation	85
	12-17 days	Predominant GGO with consolidation and increased mixed pattern	78
	18-23 days	Predominant GGO with mixed pattern	60
	$\geqslant$24 days	Predominant GGO with mixed pattern	54
Shi et al. [13]	Group 1 (<0 days)	Unilateral, multifocal GGO	15
	Group 2 ($\leqslant$7 days)	Bilateral and diffuse GGO	21
	Group 3 (8-14 days)	Predominant GGO with consolidation	30
	Group 4 (14-21 days)	Predominant GGO and reticular patterns	15
Chung et al. [23]	No change	No Changes	1
	Mild disease progression	Mild changes of opacities and density of consolidation	5
	Moderate	An increasing number of opacities	2
	disease progression	and density of consolidation	

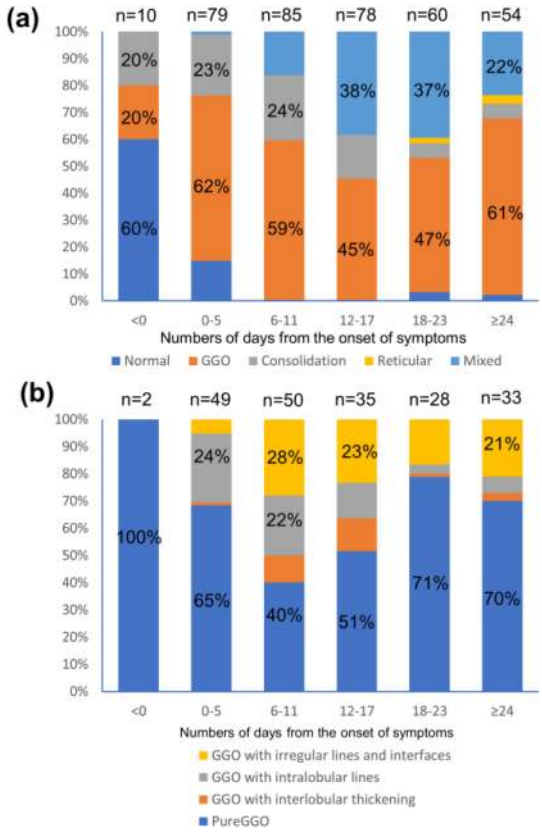

Fig. 3. Temporal changes of main CT patterns and the subtypes of GGO in [67]. (a) The distribution of CT manifestations of lung lesions; (b) the distribution of GGO subtype.

RT-PCR test [10]. With the COVID-19 patients gradually turning negative, the image manifestation also changed. CT images after recovery (RT-PCT negative) do not necessarily turn to negative at the same time, and the study suggests that CT examination is highly sensitive, but absorption is relatively slow. Li *et al.* [31] investigated the chest CT findings and clinical features associated with severe and critical COVID-19 and found that CT scores differed significantly between severe/critical and typical patients ($P < 0.001$).

Quantitative CT changes across the disease progression of COVID-19. As the disease progressed, the review conducted by Salehi *et al.* [25] suggests that progression is associated with both increased numbers and sizes of GGO combined with consolidative opacities and septal thickening, and severity can occur around 10 days after symptom onset. Liu *et al.* [61] estimated the temporal change on chest CT for pregnant women with COVID-19 using a semi-quantitative scoring system. The results showed that pregnancy and childbirth did not aggravate the course of symptoms or CT characteristics of COVID-19, and they were mostly mild type, presenting with clinical features and CT imaging progression pattern similar to those of non-pregnant women. Pan *et al.* [66] recorded the changes in CT scans of 21 RT-PCR confirmed COVID-19 patients from the initial diagnosis to recovery. The results showed that about 91% of patients reached the greatest severity (with the highest score obtained) in the peak stage (9-13 days after onset). In conclusion, the authors suggested that lung abnormalities on chest CT showed the greatest severity approximately 10 days after initial onset of symptoms. These works showed that follow-up CT characteristic analyses in a short time were feasible.

B. Remission of Lung Lesions on CT images

Several studies have described changes in CT images during the recovery process in COVID-19 infection after treatment. In a report by Liu *et al.* [68], the size of lung lesions had decreased by more than half in 67% of patients at one week after receiving antiviral and supportive treatment; this manifested on CT images as remarkable absorption and residual interstitial abnormalities with persisting septal lines. In a case report by Fang *et al.* [69], the extent and density of the patient's lung lesions had significantly decreased after 3 days of antiviral and anti-inflammatory treatment. Thus, it appears that detecting lung recovery using CT scans is feasible.

IV. AI-Based Image Analysis for COVID-19

Due to the rapid spread of COVID-19, medical resources became insufficient in many regions. Using AI to assist the disease management of COVID-19 is important. Manual diagnosis in CT scanning requires a lot of manual labor and consumes a lot of time. In order to reduce the workloads of radiologists, computer-aided diagnostic tools have been developed based on deep learning or machine learning technology. These tools have shown the potentials to increase diagnostic efficiency and reduce the pressure of radiologists (Table III).

Many recently published studies indicated that COVID-19 usually demonstrates GGO or lesions in CT images [13], [23]. Consequently, finding abnormal areas such as GGO or lesions in CT images is important for the diagnosis of COVID-19 for radiologists. Automatically detecting GGO or nodules in CT images can help reduce human effort. Chen *et al.* [70] used UNet++ [82] to extract abnormal lung areas in CT images. UNet++ is a modification of the UNet model, which is originally designed for biomedical image segmentation. Given a CT image slice, the UNet++ model can segment the areas with lesions. Afterwards, the bounding box of the segmented lesion is generated. In their study, 2D CT image slices of 106 patients (51 with COVID-19, and 55 with other diseases) were randomly divided into training and internal validation sets at the image slice-level. To predict by case, a logic linking the prediction results of consecutive images was added. CT images with the above prediction results were divided into four quadrants, and results would be output only when three consecutive images were predicted to have lesions in the same quadrant. In the internal validation set, the model correctly diagnosed the patients with a per-patient sensitivity of 100%, specificity of 93.55%, and accuracy of 95.24%. A per-image sensitivity of 94.34%, specificity of 99.16%, and accuracy of 98.85% were detected. Notably, this study used a prospective set including 27 patients for further validation, and the model achieved comparable performance to that of an expert radiologist. With the assistance of the model, the reading time of radiologists was greatly decreased by 65%.

TABLE III
COVID-19 ANALYSIS WITH CT IMAGES AND AI

Ref	Number of patients	Task	Methods	Validation	Performance
Chen et al. [70]	51 COVID-19, 82 others	COVID-19 diagnosis	UNet++	Random patient-level	ACC=0.95
Fang et al. [71]	46 COVID-19, 29 other pneumonia	COVID-19 diagnosis	Radiomic feature, consensus clustering	Random Patient-level	AUC=0.826
Wang et al. [72]	44 COVID-19 55 viral pneumonia	COVID-19 diagnosis	Manual, ResNet34, Decision tree	Random ROI level	AUC=0.78
Xu et al. [73]	110 COVID-19, 224 viral pneumonia, 175 healthy	COVID-19 diagnosis	3D CNN, 3DResNet	Random Patient-level	ACC=0.86
Jin et al. [74]	723 COVID-19, 413 others	COVID-19 diagnosis	UNet++, ResNet50	Random Patient-level	SEN=0.97 SPE=0.92
Song et al. [75]	88 COVID-19, 100 bacterial pneumonia	COVID-19 diagnosis	OpenCV, DRE-Net	Random Patient-level	AUC=0.95
Jin et al. [76]	496 COVID-19, 260 others	COVID-19 diagnosis	2D CNN	Random Patient-level	AUC=0.98
Zheng et al. [77]	313 COIVD-19, 229 others	COVID-19 diagnosis	UNet, 3DResNet	Random Patient-level	AUC=0.98
Li et al. [78]	468 COVID-19, 1,551 CAP, 1,303 others	COVID-19 diagnosis	UNet, ResNet50	Random Patient-level	AUC=0.96
Shi et al. [79]	1,658 COVID-19, 1,027 CAP	COVID-19 diagnosis	VBNet, Hand-crafted feature, Random forest	Random Patient-level	ACC=0.88
Wang et al. [80]	4,106 lung cancer, 924 COVID-19, 342 other pneumonia	COVID-19 diagnosis, prognosis	FPN, DenseNet	External Patient-level	AUC =0.87 AUC =0.88
Shi et al. [81]	151 non-severe, 45 severe	Severity diagnosis of COVID-19	V-Net, LASSO, Logistic regression	Random Patient-level	AUC=0.89

Note: ACC, AUC, SEN and SPE represent accuracy, area under the receiver operator characteristics curve, sensitivity, and specificity.

Instead of only detecting abnormal or infectious areas, an AI model that can directly diagnose COVID-19 is more convenient to use. Fang *et al.* [71] used radiomics analysis method to diagnose COVID-19. In their study, 77 radiomic features were extracted from manually delineated ROI, and unsupervised consensus clustering was used to select important features that showed a relationship with COVID-19. Finally, support vector machine (SVM) classifier was used to classify COVID-19 using the selected features. In this study, 75 patients (46 COVID-19, 29 other pneumonia) from a single center were collected, and 25 patients were randomly selected as the testing set. The radiomic model achieved an AUC of 0.826 in the testing center. Wang *et al.* [72] designed a deep-learning model to screen COVID-19 from typical viral pneumonia. Radiologists first annotated the infectious area as the region of interest (ROI). Afterwards, a modified ResNet34 was used to extract the deep learning feature, and a combination of decision tree and AdaBoost was used to classify COVID-19 and typical viral pneumonia. In the 99 patients (44 COVID-19 and 55 typical viral pneumonia patients), the model achieved an accuracy of 73.1% at the ROI-level. Since human-annotated ROIs can be affected by different users and are time-consuming, Xu *et al.* [73] proposed a deep-learning model to automatically detect infectious areas in CT images, and then used 3DResNet to identify whether the infectious areas were COVID-19. The candidate infectious regions were first segmented out using a 3D deep-learning model from a pulmonary CT image set. These separated images were then categorized into COVID-19, influenza-A viral pneumonia or healthy groups, together with the corresponding confidence scores using a location-attention classification model. Finally, the infection type and total confidence score of this CT case were calculated with noisy or Bayesian function. In the retrospective dataset (110 with COVID-19, 224 with influenza-A viral pneumonia, 175 CT samples from healthy people), 85.4% CT samples were randomly selected for training, and the rest 14.6% CT samples were used for testing. The deep-learning model achieved an accuracy of 86.7% in the testing set. Similarly, Jin *et al.* [74] developed an AI-system for COVID-19 lesion segmentation and classification. This model included three steps. First, lung regions were extracted using 3D-UNet; then, specific lesions were segmented in the lung regions; finally, a CNN-based classifier divided the lesions as being positive or negative. This system was trained with 1,136 training cases (723 positives for COVID-19) from 5 hospitals. It achieved a sensitivity of 0.974 and specificity of 0.922 in the testing set, which satisfied the requirement of clinical application.

Unlike detecting infectious regions for classification, Song *et al.* [75] extracted the whole lung area for classification. First, they extracted the main regions of the lungs and filled the blank of lung segmentation with the lung itself to avoid noise caused by different lung contours. Then, they designed a Details Relation Extraction neural network (DRE-Net) to extract the top-K details in the CT images and obtain image-level predictions. Finally, the image-level predictions were aggregated to achieve patient-level diagnoses. Eighty-eight COVID-19 and 100 bacterial pneumonia patients were used to train and validate the performance of the deep-learning model. In the testing set, the model achieved an AUC of 0.95 and a sensitivity of 0.96. Jin *et al.* [76] built a deep-learning-based diagnosis method to accelerate the speed of COVID-19 diagnosis. This deep-learning model was trained using only 312 cases' images. However, it achieved comparable performance with experienced radiologists. Among 1,255 independent testing cases, the proposed deep-learning model achieved an accuracy of 94.98%, an AUC of 97.91%, a sensitivity of 94.06%, and a specificity of 95.47%. Another reader study was conducted, and only one radiologist's performance was slightly better than this deep-learning model,

while this model could finish the diagnosis in a much shorter time.

Infectious areas can be distributed in many locations in the lungs, and automatic infectious area detection may not guarantee very high precision. Consequently, using the whole lung for classification is more convenient in practice. Zheng *et al.* [77] used UNet [83] to segment the lung area automatically, and then used 3DResNet for classification. In their dataset including 313 COVID-19 and 229 patients without COVID-19, patients were divided into a training set and a testing set according to their CT scanning time. Patients who performed CT scanning before Jan. 23, 2020 were used for training, and patients who performed CT scanning after Jan. 23, 2020 were used for testing. In the testing set including 131 patients, the deep-learning model achieved an AUC of 0.976. Similarly, Gozes *et al.* [84] used 157 patients from both China and the US as the testing set. The deep-learning model achieved an AUC of 0.996.

Due to the emergence of COVID-19, a big dataset for training and validating AI models is necessary. In Li et al's study [78], 3,506 patients (468 with COVID-19, 1,551 with Community Acquired Pneumonia (CAP), and 1,303 with non-pneumonia) were used to train and test the deep-learning model. They first used U-net to extract the whole lung region as an ROI. Afterwards, 2D RestNet50 was used for classifying COVID-19. Since each CT scanning includes multiple 2D image slices, the features in the last layer of ResNet50 were max pooled and combined for prediction. In the testing set including 1/9 randomly selected patients, the deep-learning model achieved an AUC of 0.96 in classifying COVID-19 from CAP and other pneumonia. Shi *et al.* [79] included 1658 patients with COVID-19 and 1,027 patients with CAP for classification. They first used VBNet [85] to segment infected areas, bilateral lungs, 5 lung lobes, and 18 lung pulmonary areas. Then, hand-crafted features such as infection size, location specific features and radiomic features were extracted, and least absolute shrinkage and selection operator (LASSO) was used for feature selection. Random forest was used for classification. In the five-fold validation, the method achieved a sensitivity of 0.907, a specificity of 0.833, and accuracy of 0.879. In another study, Wang *et al.* [80] proposed a fully automatic deep-learning system for COVID-19 classification and prognostic analysis. In their study, an FPN network [86] with a DenseNet121 [87] backbone was used to segment lung areas automatically. Afterwards, a network using a DenseNet structure was built to classify COVID-19 and other pneumonia. Instead of using transfer learning from natural images, they collected 4106 lung cancer patients with EGFR gene mutation status [88] to pre-train the model. Afterwards, 924 patients with COVID-19 and 342 patients with other pneumonia were used to train and validate the model. Notably, they used patients from 2 provinces in China (Heilongjiang and Anhui) for external validation. In the two independent validation sets, the deep-learning model achieved an AUC of 0.87 and 0.88. In addition, the prognostic value of the deep-learning model was explored. Features from the fully connected layer of the deep-learning model were used for prognostic feature selection. Afterwards, the Cox proportional hazard model was used to predict the hospital-stay time of patients with COVID-19. In another 2 external validation sets from Huangshi city and Beijing, the Cox model could stratify patients into high-risk and low-risk groups with different hospital-stay time ($p<0.05$, Kaplan-Meier analysis).

Except for diagnosing COVID-19, AI also shows good performance in predicting the severity of COVID-19. Shi *et al.* [81] proposed a deep-learning-based quantitative assessment method to predict the severity of COVID-19 (severe vs. non-severe). The deep learning method calculated two indices named mass of infection (MOI) and the percentage of infection (POI), which had higher values in the severe group than the non-severe group of patients. Then, the LASSO logistic regression model combined POI and MOI with clinical features such as age, lactate dehydrogenase (LDH), C-reactive protein (CRP) and CD4+ T cell counts to classify the patients as severe patients or non-severe patients. The AUC in the testing dataset achieved 0.89, which was significantly higher than the baseline pneumonia severity index. Current studies indicated that AI shows good performance in quickly diagnosing COVID-19. With the assistance of AI, clinicians can be separated from patients to avoid infection. On the other hand, CT image is easy to acquire. Using AI and CT images to diagnose COVID-19 does not add an additional cost.

V. Discussion

The COVID-19 pandemic has rapidly become a major global health threat. Imaging techniques, in particular CT, play a critical role in diagnosis and monitoring COVID-19 pneumonia. In the majority of current studies, CT remains the primary tool for assessing lung lesions in COVID-19 cases, and evaluating changes in the severity of lung lesions. With the progression of CIVID-19, different degrees of lung lesions can be observed by multiple CT scans.

The most common CT manifestation of COVID-19 is GGO, followed by consolidation. With the advance of the disease, a decrease in GGO and an increase in consolidation can be observed. In addition, pure GGO also gradually becomes more diversified CT features including crazy-paving pattern, reticular pattern, vacuolar sign, fibrotic streaks, a subpleural line, a subpleural transparent line, air bronchogram, and bronchus distortion in this process. However, the clinical manifestations can vary between patients, which helps to explain some discrepancies between different studies. Changes in lung lesions are closely related to the disease progression of COVID-19. For example, patients with rapid disease progression also exhibit a rapid enlargement of lung lesions on CT imaging within 24-48 hours. The response to treatment also varies between patients. In most patients with mild disease, the lung lesions are absorbed after receiving treatment. However, lung lesions of patients with the severe or critical diseases may be irreversible. Current studies on the follow-up CT scans for COVID-19 are still dealing with a small number of samples. Additional research, ideally multi-center data with large sample sizes, is needed to provide further insights into the evolution of lung lesions during and after an infection caused by COVID-19.

In the clinical diagnosis of COVID-19, chest CT can supplement RT-PCR testing and compensate for its relatively poor

sensitivity. Ai *et al.* [10] compared the diagnostic value and consistency of chest CT scans and RT-PCR results from the swab samples of 1,014 patients in the epidemic area of China, all of whom had undergone both chest CT and RT-PCR testing. They demonstrated a higher sensitivity of chest CT than of RT-PCR for the diagnosis of COVID-19. With the RT-PCR results as a reference, the sensitivity, specificity, and accuracy of chest CT in determining SARS-CoV-2 infection were 97%, 25%, and 68%, respectively. The PPV and NPV were 65% and 83%, respectively. Moreover, Fu *et al.* [11] analyzed the data of 52 patients with COVID-19 who had been discharged and found heterogeneity between chest CT findings and RT-PCR results, especially in some of the recovered patients with negative RT-PCR results. Some patients with COVID-19 will have negative RT-PCR results, and yet they can still exhibit inflammatory changes that are visible on chest CT images [12]. Thus, chest CT combined with epidemiological history and laboratory tests is useful for detecting COVID-19 and evaluating progression and treatment effects [89]. However, it is important to note that Guan *et al.* [5] reported that many patients do not exhibit abnormal radiologic findings, and such patients should not be overlooked in the screening and diagnosis of COVID-19. For asymptomatic patients, especially for those who showed normal CT findings without any clinical symptoms, the combination of chest CT imaging, RT-PCR, epidemiological history, and close follow-up is highly recommended to confirm these asymptomatic COVID-19 patients.

Due to the emergent nature of COVID-19, the medical resources in many parts of the world are insufficient. Quickly diagnosing COVID-19 and predicting individualized prognosis are important for the management of COVID-19. Recent studies have reported promising results of the use of AI combined with CT imaging, which can assist in the rapid diagnosis of COVID-19 and prognostic predictions. As CT images exhibit several prognostic and diagnostic characteristics of COVID-19, the rapid and precise quantification of these characteristics using AI has garnered considerable attention. Three types of AI strategies have been reported: 1) use AI to detect lesions to assist fast screening of COVID-19 for clinicians; 2) use AI to diagnose COVID-19 using partial or whole lung in CT images; 3) use AI to predict other clinical outcomes of COVID-19 (e.g., the severity of COVID-19). Among the studies using deep learning for diagnosing COVID-19, UNet and its modifications were often used for segmenting lung or lesions from CT images, and ResNet (2D or 3D) were often used for classification. Compared with studies using segmented lung lesions for classification, using the whole lung for analysis achieved similar results, which may suggest that segmenting or detecting lung lesions for analysis may not be necessary. Since lesion segmentation is more difficult than lung segmentation, and multiple lesions or infectious areas can exist in lung, using the whole lung for analysis is more reasonable and convenient.

Despite promising results in recent studies [71], [81], many AI models were tested in small datasets. The studies using the small dataset (e.g., $<$300 patients) often showed high AUC or accuracy. However, in several studies with the larger dataset ($>$ 1000 patients) [13], [80], the performance drops. Consequently, the very high accuracy of AI models in a small dataset may be caused by overfitting. The larger-scale studies with lower accuracy may reflect the real ability of what AI could achieve in diagnosing COVID-19. On the other hand, very few studies used independent and external validation dataset to evaluate the generalization ability of deep learning models. In the future, a large external validation dataset should be used. Due to the limited training data of COVID-19, transfer learning using chest CT images could be a good strategy. In [80], the CNN model was first trained using a lung cancer dataset including 4106 patients, and finally achieved good performance in diagnosing COVID-19. Many transfer learning models in current studies used ResNet that was pre-trained in ImageNet dataset. Using chest CT image for transfer learning may be a better choice, such as using the LIDC-IDRI dataset for pre-training. In addition, many of the previous studies on AI have focused on the rapid diagnosis of COVID-19. However, the prognostic analysis of COVID-19 is essential to the management of COVID-19, and combined AI and CT imaging can play an important role in treatment and management. For example, AI and CT can be used to identify patients with a high risk of progressing to severe disease or even of death; it can also be used to evaluate or predict the response of specific therapies.

Although CT is the primary tool for screening and evaluating disease severity in patients with COVID-19, other clinical imaging methods, such as PET, MRI, and ultrasound, have also added value by identifying specific imaging features that can be used for the diagnosis of pneumonia. These clinical imaging tools can be used as a complement to chest CT in the examination of COVID-19 pneumonia, especially for patients with comorbidities. MRI plays a key role in pediatric examinations and evaluating cardiac involvement of COVID-19. PET can be used for reviewing inflammatory and infectious pulmonary diseases. In addition, PET is a promising imaging tool in monitoring disease progression and treatment effects to improve patient management. Additionally, LUS has also shown potential in the examination and management of COVID-19. It is especially suitable for screening pregnant women and children and for patients admitted to ICU, due to being radiation-free, low-cost, and portable. However, LUS results may vary with different operators. Guidelines for LUS examinations of COVID-19 pneumonia should be developed as soon as possible.

COVID-19 is highly transmissible, pathogenic, and deadly, especially in the elderly and patients with underlying diseases. Meanwhile, it is also very occult in terms of clinical symptoms. Individual differences in clinical symptoms and laboratory indicators (C-reactive protein, lymphocytes) of patients increase in the acute phase, and decrease or return to normal in the recovery phase. Altough Ai et al.'s report [10] highlighted the sensitivity of chest CT in COVID-19 diagnosis, Raptis *et al.* [90] have presented that Ai et al.'s study might overestimate the sensitivity of CT at the expense of specificity. Therefore, epidemiology, nucleic acid detection results, CT image features, clinical symptoms, and laboratory indicators should be taken into consideration to make a comprehensive and objective assessment, so as to prevent a missed diagnosis or misdiagnosis and effectively improve the clinical effects.

VI. Conclusion

In summary, various imaging technologies can play important roles in the management of COVID-19. Nucleic acid testing remains the gold standard of clinical diagnosis. However, imaging characteristics, especially those of CT scans, can reflect lung parenchyma changes, bronchial changes, and pleural changes. Typical CT signs of COVID-19 include GGO, consolidation, vascular enlargement, and pleural thickening. The majority of cases show bilateral involvement and multiple mottling. The joint use of these imaging biomarkers and RT-PCR testing can improve COVID-19 screening and diagnosis. The findings of this review suggest that COVID-19 diagnosis should be based on epidemiological history, nucleic acid detection, CT imaging, clinical symptoms and signs, and laboratory findings. The combined use of AI and CT imaging can offset limitations in medical resources, as well as support the rapid diagnosis and prognostic prediction of COVID-19.

Though the follow-up CT studies for COVID-19 is still limited for now, common changing pattern of lung lesions can still be observed, which includes appearance of GGO in the relatively early stages and increased consolidation with the advance of disease. In process of remission, the recovery patterns are mostly manifested as lesion absorbing. CT scans have proved as an efficient clinical tool in assessing the progression and remission of lung lesions in COVID-19 infection. Multi-center studies with large sample-size are still needed to ascertain the current findings.

References

[1] J. F. Chan *et al.*, "A familial cluster of pneumonia associated with the 2019 novel coronavirus indicating person-to-person transmission: A study of a family cluster," *Lancet*, vol. 395, no. 10223, pp. 514–523, Feb. 15, 2020.

[2] N. Zhu *et al.*, "A novel Coronavirus from patients with Pneumonia in China, 2019," *N. Engl. J. Med.*, vol. 382, no. 8, pp. 727–733, 2020.

[3] N. Chen *et al.*, "Epidemiological and clinical characteristics of 99 cases of 2019 novel coronavirus pneumonia in Wuhan, China: A descriptive study," *Lancet North Am. Ed.*, vol. 395, no. 10223, pp. 507–513, 2020.

[4] X. Yang, Y. Yu, and J. Xu, "Clinical course and outcomes of critically ill patients with SARS-CoV-2 pneumonia in Wuhan, China: A single-centred, retrospective, observational study," *Lancet Respiratory Med.*, vol. 8, no. 4, pp. 475–481, Apr 2020.

[5] W.-j. Guan *et al.*, "Clinical characteristics of Coronavirus disease 2019 in China," *N. Engl. J. Med.*, vol. 382, no. 18, pp. 1708–1720, 2020.

[6] Z. Wu and J. M. McGoogan, "Characteristics of and important lessons from the Coronavirus disease 2019 (COVID-19) outbreak in China: Summary of a report of 72 314 cases from the Chinese Center for Disease Control and Prevention," *JAMA*, vol. 323, no. 13, pp. 1239–1242, 2020.

[7] M. D. Hope, C. A. Raptis, and T. S. Henry, "Chest computed tomography for detection of Coronavirus disease 2019 (COVID-19): Don't Rush the Science," *Ann. Intern. Med.*, 2020.

[8] "Clinical management of severe acute respiratory infection when Novel coronavirus (2019-nCoV) infection is suspected: Interim Guidance," *World Health Organization*.

[9] *National Health Commission of the People's Republic of China, Diagnosis and treatment protocol for COVID-19 (trial version 7)*. [Online]. Available: http://en.nhc.gov.cn/2020-03/29/c_78469.htm

[10] T. Ai *et al.*, "Correlation of chest CT and RT-PCR testing in coronavirus disease 2019 (COVID-19) in China: A report of 1014 cases," *Radiology*, p. 200642, 2020.

[11] H. Fu *et al.*, "Association between clinical, laboratory and CT characteristics and RT-PCR results in the follow-up of COVID-19 patients," *medRxiv*, 2020.

[12] X. Xie, Z. Zhong, W. Zhao, C. Zheng, F. Wang, and J. Liu, "Chest CT for typical 2019-nCoV pneumonia: Relationship to negative RT-PCR testing," *Radiology*, p. 200343, 2020.

[13] H. Shi *et al.*, "Radiological findings from 81 patients with COVID-19 pneumonia in Wuhan, China: A descriptive study," *The Lancet. Infectious diseases*, Feb. 24, 2020.

[14] J. P. Kanne, "Chest CT findings in 2019 novel Coronavirus (2019-nCoV) infections from Wuhan, China: Key Points for the Radiologist," *Radiology*, vol. 295, no. 1, pp. 16–17, Apr. 2020.

[15] Z. Ye, Y. Zhang, Y. Wang, Z. Huang, and B. Song, "Chest CT manifestations of new coronavirus disease 2019 (COVID-19): A pictorial review," *Eur. Radiol.*, pp. 1–9, 2020.

[16] A. J. Rodriguez-Morales *et al.*, "Clinical, laboratory and imaging features of COVID-19: A systematic review and meta-analysis," *Travel Medicine and Infectious Disease*, vol. 34, p. 101623, Mar. 2020.

[17] D. Wang *et al.*, "Clinical characteristics of 138 hospitalized patients with 2019 novel coronavirus–infected pneumonia in Wuhan, China," *JAMA*, 2020.

[18] A. Bernheim *et al.*, "Chest CT findings in Coronavirus disease-19 (COVID-19): Relationship to duration of infection," *Radiology*, pp. 200463–200463, Feb. 20, 2020.

[19] L. L. Zhang, D. N. C. Wang, Q. H. Huang, and X. D. Wang, "Significance of clinical phenomes of patients with COVID-19 infection: A learning from 3795 patients in 80 reports," *Clin. Transl. Med.*, 2020.

[20] J. Liu, H. Yu, and S. Zhang, "The indispensable role of chest CT in the detection of coronavirus disease 2019 (COVID-19)," (in eng), *Eur. J. Nucl. Med. Mol. Imaging*, pp. 1–2, 2020.

[21] Y.-H. Jin *et al.*, "A rapid advice guideline for the diagnosis and treatment of 2019 novel coronavirus (2019-nCoV) infected pneumonia (standard version)," *Military Med. Res.*, vol. 7, no. 1, p. 4, 2020.

[22] H. Liu, F. Liu, J. Li, T. Zhang, D. Wang, and W. Lan, "Clinical and CT imaging features of the COVID-19 Pneumonia: Focus on pregnant women and children," *J. Infect.*, vol. 80, no. 5, pp. 7–13, Mar. 11, 2020.

[23] M. Chung *et al.*, "CT imaging features of 2019 novel Coronavirus (2019-nCoV)," *Radiology*, vol. 295, no. 1, pp. 202–207, Apr. 2020.

[24] R. Han, L. Huang, H. Jiang, J. Dong, H. Peng, and D. Zhang, "Early clinical and CT manifestations of Coronavirus disease 2019 (COVID-19) Pneumonia," *Am. J. Roentgenol.*, pp. 1–6, 2020.

[25] S. Salehi, A. Abedi, S. Balakrishnan, and A. Gholamrezanezhad, "Coronavirus disease 2019 (COVID-19): A systematic review of imaging findings in 919 patients," (in eng), *AJR Am J Roentgenol*, pp. 1–7, Mar. 14 2020.

[26] Y. H. Xu *et al.*, "Clinical and computed tomographic imaging features of novel coronavirus pneumonia caused by SARS-CoV-2," *J. Infect.*, vol. 80, no. 4, pp. 394–400, Apr 2020.

[27] J. Wu *et al.*, "Chest CT findings in patients with corona virus disease 2019 and its relationship with clinical features," *Invest. Radiol.*, vol. 55, no. 5, pp. 257–261, 2020.

[28] W. Zhao, Z. Zhong, X. Xie, Q. Yu, and J. Liu, "Relation between chest CT findings and clinical conditions of coronavirus disease (COVID-19) pneumonia: A multicenter study," *Am. J. Roentgenol.*, vol. 214, no. 5, pp. 1072–1077, 2020.

[29] H. X. Bai *et al.*, "Performance of radiologists in differentiating COVID-19 from viral pneumonia on chest CT," *Radiology*, vol. 0, no. 0, p. 200823, 2020.

[30] W. Zhu, K. Xie, H. Lu, L. Xu, S. Zhou, and S. Fang, "Initial clinical features of suspected Coronavirus disease 2019 in two emergency departments outside of Hubei, China," *J. Med. Virol.*, Mar. 2020.

[31] K. Li *et al.*, "The clinical and chest CT features associated with severe and critical COVID-19 pneumonia," *Invest. Radiol.*, vol. 55, no. 6, pp. 327–331, 2020.

[32] C. Huang *et al.*, "Clinical features of patients infected with 2019 novel coronavirus in Wuhan, China," *Lancet*, vol. 395, no. 10223, pp. 497–506, Feb. 15 2020.

[33] F. Song *et al.*, "Emerging 2019 novel coronavirus (2019-nCoV) pneumonia," *Radiology*, vol. 295, no. 1, pp. 210–217, 2020.

[34] P. Sun, S. Qie, Z. Liu, J. Ren, K. Li, and J. Xi, "Clinical characteristics of 50466 hospitalized patients with 2019-nCoV infection," *J. Med. Virol.*, vol. 92, no. 6, pp. 612–617, 2020.

[35] S. Zhou, Y. Wang, T. Zhu, and L. Xia, "CT features of Coronavirus disease 2019 (COVID-19) Pneumonia in 62 patients in Wuhan, China," *Am. J. Roentgenol.*, vol. 0, no. 0, pp. 1–8, 2020.

[36] W. Hao and M. Li, "Clinical diagnostic value of CT imaging in COVID-19 with multiple negative RT-PCR testing," *Travel Medicine and Infectious Disease*, vol. 34, p. 101627, 2020.

[37] Y. Fang *et al.*, "Sensitivity of chest CT for COVID-19: Comparison to RT-PCR," *Radiology*, vol. 0, no. 0, p. 200432, 2020.

[38] Z. Hu *et al.*, "Clinical characteristics of 24 asymptomatic infections with COVID-19 screened among close contacts in Nanjing, China," *Sci. China Life Sci.*, vol. 63, no. 5, pp. 706–711, 2020.

[39] Z. Ling *et al.*, "Asymptomatic SARS-CoV-2 infected patients with persistent negative CT findings," *Eur. J. Radiol.*, vol. 126, p. 108956, 2020.

[40] L. A. Marinari, M. A. Danny, and W. T. Miller, "Sporadic coronavirus lower respiratory tract infection in adults: Chest CT imaging features and comparison with other viruses," *Eur. Respir. J.*, vol. 54, Sep. 2019.

[41] D. Zhao *et al.*, "A comparative study on the clinical features of COVID-19 pneumonia to other pneumonias," *Clin. Infect. Dis.*, Mar. 2020.

[42] C. Qin, F. Liu, T.-C. Yen, and X. Lan, "F-18-FDG PET/CT findings of COVID-19: a series of four highly suspected cases," *Eur. J. Nucl. Med. Mol. Imaging*, vol. 47, no. 5, pp. 1281–1286, 2020.

[43] S. Zou and X. Zhu, "FDG PET/CT of COVID-19," *Radiology*, p. 200770, Mar. 6 2020.

[44] K. M. Das, E. Y. Lee, R. D. Langer, and S. G. Larsson, "Middle east respiratory syndrome coronavirus: what does a radiologist need to know?," *Am. J. Roentgenol.*, vol. 206, no. 6, pp. 1193–1201, 2016.

[45] Y. Deng, L. Lei, Y. Chen, and W. Zhang, "The potential added value of FDG PET/CT for COVID-19 pneumonia," (in eng), *Eur. J. Nucl. Med. Mol. Imaging*, pp. 1–2, Mar. 21, 2020.

[46] H. Chu *et al.*, "Comparative replication and immune activation profiles of SARS-CoV-2 and SARS-CoV in human lungs: An ex vivo study with implications for the pathogenesis of COVID-19," *Clin. Infect. Dis.*, 2020.

[47] B. Joob and V. Wiwanitkit, "18F-FDG PET/CT and COVID-19," *Eur. J. Nucl. Med. Mol. Imaging*, pp. 1–1, 2020.

[48] G. Soldati *et al.*, "Is there a role for lung ultrasound during the COVID-19 pandemic?," *J. Ultrasound Medicine: Official J. Amer. Inst. Ultrasound Medicine*, Mar. 20, 2020.

[49] E. Poggiali *et al.*, "Can lung US help critical care clinicians in the early diagnosis of novel Coronavirus (COVID-19) Pneumonia?," *Radiology*, p. 200847, 2020.

[50] E. Kalafat *et al.*, "Lung ultrasound and computed tomographic findings in pregnant woman with COVID-19," (in eng), *Ultrasound Obstet. Gynecol.*, Apr. 6, 2020.

[51] Q. Y. Peng, X. T. Wang, L. N. Zhang, and G. Chinese Critical Care Ultrasound Study, "Findings of lung ultrasonography of novel corona virus pneumonia during the 2019-2020 epidemic," *Intensive Care Med*, vol. 46, no. 5, pp. 849–850, 2020.

[52] D. Buonsenso, A. Piano, F. Raffaelli, N. Bonadia, K. de Gaetano Donati, and F. Franceschi, "Point-of-Care lung ultrasound findings in novel coronavirus disease-19 pnemoniae: A case report and potential applications during COVID-19 outbreak," *Eur. Rev. Med. Pharmacol. Sci.*, vol. 24, no. 5, pp. 2776–2780, 2020-03 2020.

[53] F. Moro *et al.*, "How to perform lung ultrasound in pregnant women with suspected COVID-19 infection," *Ultrasound Obstet. Gynecol.*, vol. 55, no. 5, pp. 593–598, 2020.

[54] M. C. Liszewski, S. Gorkem, K. S. Sodhi, and E. Y. Lee, "Lung magnetic resonance imaging for pneumonia in children," *Pediatr. Radiol.*, vol. 47, no. 11, pp. 1420–1430, Oct. 2017.

[55] X. H. Yao *et al.*, "A pathological report of three COVID-19 cases by minimally invasive autopsies," *Zhonghua Bing Li Xue Za Zhi*, vol. 49, no. 0, p. E009, Mar. 15 2020.

[56] L. Chen, X. Li, M. Chen, Y. Feng, and C. Xiong, "The ACE2 expression in human heart indicates new potential mechanism of heart injury among patients infected with SARS-CoV-2," *Cardiovasc Res.*, Mar. 30, 2020.

[57] R. M. Inciardi *et al.*, "Cardiac involvement in a patient with Coronavirus disease 2019 (COVID-19)," *JAMA Cardiol.*, Mar. 27, 2020.

[58] X. Zou, K. Chen, J. Zou, P. Han, J. Hao, and Z. Han, "Single-cell RNA-seq data analysis on the receptor ACE2 expression reveals the potential risk of different human organs vulnerable to 2019-nCoV infection," *Front Med*, Mar. 12, 2020.

[59] H. Syrjala, M. Broas, P. Ohtonen, A. Jartti, and E. Paakko, "Chest magnetic resonance imaging for pneumonia diagnosis in outpatients with lower respiratory tract infection," *Eur Respir J*, vol. 49, no. 1, Jan. 2017.

[60] P. Konietzke *et al.*, "The value of chest magnetic resonance imaging compared to chest radiographs with and without additional lung ultrasound in children with complicated pneumonia," *PLoS One*, vol. 15, no. 3, p. e0230252, 2020.

[61] D. Liu *et al.*, "Pregnancy and perinatal outcomes of women with Coronavirus disease (COVID-19) Pneumonia: A preliminary analysis," *AJR. Am. J. Roentgenol.*, pp. 1–6, Mar. 18, 2020.

[62] J. C. L. Rodrigues *et al.*, "An update on COVID-19 for the radiologist - A British society of thoracic imaging statement," *Clin. Radiol.*, vol. 75, no. 5, pp. 323–325, Mar. 23, 2020.

[63] M.-Y. Ng *et al.*, "Imaging profile of the COVID-19 infection: Radiologic findings and literature review," *Radiol.: Cardiothoracic Imaging*, vol. 2, no. 1, 2020.

[64] R. Yang *et al.*, "Chest CT severity score: An imaging tool for assessing severe COVID-19," *Radiol.: Cardiothoracic Imaging*, vol. 2, no. 2, p. e200047, 2020.

[65] M. Li *et al.*, "Coronavirus disease (COVID-19): Spectrum of CT findings and temporal progression of the disease," *Acad. Radiol.*, vol. 27, no. 5, pp. 603–608, 2020.

[66] F. Pan *et al.*, "Time course of lung changes on chest CT during recovery from 2019 novel Coronavirus (COVID-19) Pneumonia," *Radiology*, pp. 200370–200370, 2020-Feb-12 2020.

[67] Y. Wang *et al.*, "Temporal changes of CT findings in 90 patients with COVID-19 Pneumonia: A longitudinal study," *Radiology*, pp. 200843–200843, Mar. 19, 2020.

[68] K.-C. Liu *et al.*, "CT manifestations of coronavirus disease-2019: A retrospective analysis of 73 cases by disease severity," *Eur. J. Radiol.*, vol. 126, pp. 108941–108941, Mar. 12, 2020.

[69] X. Fang, M. Zhao, S. Li, L. Yang, and B. Wu, "Changes of CT findings in a 2019 Novel Coronavirus (2019-nCoV) pneumonia patient," *QJM: Monthly J. Association Physicians*, vol. 113, no. 6, pp. 271–272, 2020.

[70] J. Chen *et al.*, "Deep learning-based model for detecting 2019 novel coronavirus pneumonia on high-resolution computed tomography: A prospective study," 2020, *medRxiv*: 2020.02.25.20021568.

[71] M. FANG *et al.*, "CT radiomics can help screen the coronavirus disease 2019 (COVID-19): A preliminary study," *SCI. CHINA Inf. Scie.*, vol. 63, no. 1674-733X, p. 172103, 2020.

[72] S. Wang *et al.*, "A deep learning algorithm using CT images to screen for Corona Virus Disease (COVID-19)," 2020, *medRxiv:* 2020.02.14.20023028.

[73] X. Xu *et al.*, "Deep learning system to screen Coronavirus disease 2019 Pneumonia," 2020, *arXiv: 2002.09334*.

[74] S. Jin *et al.*, "AI-assisted CT imaging analysis for COVID-19 screening: Building and deploying a medical AI system in four weeks," 2020, *medRxiv:* 2020.03.19.20039354.

[75] Y. Song *et al.*, "Deep learning Enables Accurate Diagnosis of Novel Coronavirus (COVID-19) with CT images," 2020, *medRxiv*: 2020.02.23.20026930.

[76] C. Jin *et al.*, "Development and evaluation of an AI system for COVID-19 diagnosis," 2020, *medRxiv:* 2020.03.20.20039834.

[77] C. Zheng *et al.*, "Deep learning-based detection for COVID-19 from chest CT using weak label," 2020, *medRxiv:* 2020.03.12.20027185,.

[78] L. Li *et al.*, "Artificial intelligence distinguishes COVID-19 from community acquired Pneumonia on chest CT," *Radiology*, p. 200905, 2020.

[79] F. Shi *et al.*, "Large-scale screening of COVID-19 from community acquired Pneumonia using infection size-aware classification,"2020, *arXiv: 2003.09860*.

[80] S. Wang *et al.*, "A fully automatic deep learning system for COVID-19 diagnostic and prognostic analysis," 2020, *medRxiv*: 2020.03.24.20042317.

[81] W. Shi *et al.*, "Deep learning-based quantitative computed tomography model in predicting the severity of COVID-19: A retrospective study in 196 patients," *SSRN Electron. J.*, Jan. 1, 2020.

[82] Z. Zhou, M. M. R. Siddiquee, N. Tajbakhsh, and J. Liang, "Unet++: A nested u-net architecture for medical image segmentation," in *Deep Learning in Medical Image Analysis and Multimodal Learning for Clinical Decision Support*: Springer, 2018, pp. 3–11.

[83] O. Ronneberger, P. Fischer, and T. Brox, "U-net: Convolutional networks for biomedical image segmentation," in *Int. Conference on Medical Image Computing Computer-Assisted Intervention*, 2015, pp. 234–241: Springer.

[84] O. Gozes *et al.*, "Rapid ai development cycle for the coronavirus (covid-19) pandemic: Initial results for automated detection & patient monitoring using deep learning ct image analysis," 2020, *arXiv:2003.05037*.

[85] F. Shan *et al.*, "Lung Infection Quantification of COVID-19 in CT Images with Deep Learning," 2020, *arXiv:2003.04655*.

[86] T.-Y. Lin, P. Dollár, R. Girshick, K. He, B. Hariharan, and S. Belongie, "Feature pyramid networks for object detection," in *Proc. IEEE Conf. Comput. Vision Recognit.*, pp. 2117–2125, 2017.

[87] G. Huang, Z. Liu, L. Van Der Maaten, and K. Q. Weinberger, "Densely connected convolutional networks," in *Proc. IEEE Comput. Vision Pattern Recognit.*, pp. 4700–4708, 2017.

[88] S. Wang*et al.*, "Predicting EGFR mutation status in lung adenocarcinoma on computed tomography image using deep learning," *Eur. Respir. J.*, vol. 53, no. 3, p. 1800986, 2019.
[89] X. Zhao*et al.*, "The characteristics and clinical value of chest CT images of novel coronavirus pneumonia," *Clin. Radiol.*, vol. 75, no. 5, pp. 335–340, May 2020.
[90] C. A. Raptis*et al.*, "Chest CT and Coronavirus disease (COVID-19): A critical review of the literature to date," *Am. J. Roentgenol.*, pp. 1–4, 2020.

Di Dong received the Ph.D. degree in pattern recognition and intelligent systems from the Institute of Automation, Chinese Academy of Sciences, China, in 2013. He is currently an Associate Professor with the Institute of Automation, Chinese Academy of Sciences. He is the member of the Youth Innovation Promotion Association of the Chinese Academy of Sciences. He has carried out long-term research work in the field of radiomics and medical big data analysis. In recent years, he has published nearly 50 peer-reviewed SCI journal papers, among which six papers are ESI highly cited papers.

Zhenchao Tang received the B.S. degree from the School of Information Science and Engineering, Shandong University, in 2012, and the Ph.D. degree from the School of Mechanical, Electrical & Information Engineering, Shandong University, in 2019. He is currently a Postdoc with Beijing Advanced Innovation Center for Big Data-Based Precision Medicine, School of Medicine and Engineering, Beihang University. His current research interests including medical images processing and deep learning.

Shuo Wang received the Ph.D. degree in pattern recognition and intelligent systems from the Institute of Automation, Chinese Academy of Sciences, China, in 2019. He is currently a Postdoctor with the School of Medicine and Engineering, Beihang University. He has carried out long-term research work in the field of deep learning and medical image analysis, especially in lung cancer analysis based on deep learning. Related works were published in *European Respiratory Journal, Medical Image Analysis, Theranostics, and Radiotherapy and Oncology*, etc.

Hui Hui received the B.S. and M.S. degrees in mechanical engineering from the Chang'an University, China, in 2003 and 2006 respectively, and the Ph.D. degree in mechanical engineering from the University of Franche-Comté, France, in 2013. He is currently an Associate Professor with the Institute of Automation, Chinese Academy of Sciences. He is the member of the Youth Innovation Promotion Association of the Chinese Academy of Sciences. His current research interests include multimodal molecular imaging and optical microscopy.

Lixin Gong received the M.S. degree in biomedical engineering from the College of Medicine and Biological Information Engineering, School of Northeastern University, China, in 2018. She is currently working toward the Ph.D. degree at the College of Medicine and Biological Information Engineering School of Northeastern University, majoring in biomedical engineering. She. Her current research interests include tumor radiomics and medical big data analysis.

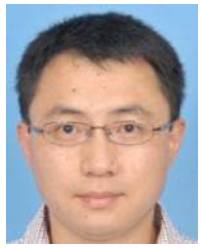

Yao Lu received the bachelor's degree in mathematics from the University of Science and Technology of China, Hefei, China, the master's degree from the Institute of Mathematics, Chinese Academy of Sciences, and the Ph.D. degree in mathematics from Syracuse University, Syracuse, NY, USA. He is currently a Full Professor with the School of Data Science and Computer Science, Sun Yat-sen University, Guangzhou, China. Prior to joining Sun Yat-sen University, he was a Research Investigator with the Department of Radiology, University of Michigan, Ann Arbor, MI, USA. His research interests are in image processing, medical image analysis, and ill-posed problems.

Zhong Xue, photograph and biography not available at the time of publication.

Hongen liao, photograph and biography not available at the time of publication.

Fang Chen, photograph and biography not available at the time of publication.

Fang Yang, photograph and biography not available at the time of publication.

Ronghua Jin, photograph and biography not available at the time of publication.

Kun Wang, photograph and biography not available at the time of publication.

Zhenyu Liu, photograph and biography not available at the time of publication.

Jingwein Wei, photograph and biography not available at the time of publication.

Wei Mu, photograph and biography not available at the time of publication.

Hui Zhang, photograph and biography not available at the time of publication.

Jingying Jiang, photograph and biography not available at the time of publication.

Jie Tian received the Ph.D. degree (with honors) in artificial intelligence from the Chinese Academy of Sciences, in 1993. Since 1997, he has been a Professor with the Chinese Academy of Sciences. He has been elected as the Fellow of ISMRM, AIMBE, IAMBE, IEEE, OSA, SPIE, and IAPR. He serves as the Editorial Board Member of *Molecular Imaging and Biology, European Radiology*, IEEE TRANSACTIONS ON MEDICAL IMAGING, IEEE TRANSACTIONS ON BIOMEDICAL ENGINEERING, IEEE JOURNAL OF BIOMEDICAL AND HEALTH INFORMATICS, and Photoacoustics. He is the Author of over 400 peer-reviewed journal articles, including publication in *Nature Biomedical Engineering, Science Advances, Journal of Clinical Oncology, Nature Communications, Radiology*, and many other journals, and these articles received over 25,000 Google Scholar citations (H-index 79). He is recognized as a Pioneer and a Leader in China in the field of molecular imaging. In the last two decades, he has developed a series of new optical imaging models and reconstruction algorithms for in vivo optical tomographic imaging. He has developed new artificial intelligence strategies for medical imaging big data analysis in the field of Radiomics, and played a major role in establishing a standardized Radiomics database with more than 100,000 cancer patients data collected from over 50 hospitals all over China. He has received numerous awards, including five national top awards for his outstanding work in medical imaging and biometrics recognition.

Hongjun Li is a Senior Doctor in Capital Medical University. He is an Expert in medical imaging of legal infectious diseases. He is the Leader of the science referred as 'Radiology of infectious diseases' (praised by Prof. Garry Gold, a famous Top-Radiologist worldwide who is specialized in MRI and works in Stanford University). He had led the Chinese Radiology Society in infectious diseases to advance in clinical research, technological development, publications, educations, and clinical practices in AIDS, inflammatory, Tuberculosis, and other emerging infectious diseases.